



Project Deliverable D5.3

Project Number: 325275	Project Acronym: SAPPHIRE	Project Title: System Automation of PEMFCs with Prognostics and Health management for Improved Reliability and Economy
Instrument: Collaborative Project (CP)		Thematic Priority FUEL CELL AND HYDROGEN JOINT UNDERTAKING
Title: Condition monitoring and health assessment of PEM fuel cells		
Contractual Delivery Date: April 30, 2015		Actual Delivery Date: July 24, 2015
Start date of project: May 1, 2013		Duration: 36 months
Organisation name of lead contractor for this deliverable: FESB, University of Split		Document version: Version 1.2
Organisation notes:		

Dissemination level (Project co-funded by the European Commission within the Seventh Framework Programme)		
PU	Public	PU Public
PP	Restricted to other programme participants (including the Commission)	
RE	Restricted to a group defined by the consortium (including the Commission)	
CO	Confidential, only for members of the consortium (including the Commission)	



Authors (organizations):

Dario Bezmalinovic, FESB, University of Split

Frano Barbir, FESB, University of Split

Abstract :

A novel equivalent circuit model is made by adding additional resonance loops comprising of a resistance, capacitance and inductance, for both anode and cathode, representing mass transport and resistive losses within the catalyst layer. Such a model is able to match and explain low frequency inductance observed in all Electrochemical Impedance Spectroscopy measurements taken during durability tests. The model was used to monitor the state of health of a fuel cell exposed to a controlled accelerated stress test. The results indicate that resistance, capacitance and inductance representing the cathode catalyst layer change dramatically during the accelerated stress test, and this shows good agreement with the findings of the periodic diagnostic tests.

Keywords: electrochemical impedance spectroscopy, equivalent circuit model, low frequency inductance,

Revision History

Rev.	Date	Description	Author (Organisation)
1.0	17.07.2015.	1 st Draft	Dario Bezmalinovic
1.1	22.07.2015.	2 nd Draft	Frano Barbir
1.2	24.07.2015.	Final Submission	Frano Barbir



Condition monitoring and health assessment of PEM fuel cells

1. Introduction

Electrochemical impedance spectroscopy (EIS) is a well-known method for modeling and diagnosis of PEM fuel cells, which enables in-situ identification and quantification of physical phenomena that influence fuel cell performance and degradation [1-4].

One feature of the impedance spectra that is less researched and understood is inductance loop at low frequencies. Impedance spectra typically exhibit inductive features at high frequencies, while some authors report inductive loops also at low frequencies. The high-frequency inductive features are understood to be caused by wiring and instrument artifacts, but the interpretation of the low-frequency inductive loops is less clear. Several possible explanations for the low-frequencies loop have been proposed: adsorption-desorption phenomena in heterogeneous reactions [5], presence of an adsorbed intermediate in the rate controlling step [5,6], Pt dissolution and associated deactivation of catalytic activity [7], slow response of CO coverage to the changes in electrode potential [8], limited supply of dissolved oxygen within the narrow pores [9], water transport characteristics in the membrane [10], rehydration of the membrane and the anode by product water from the oxygen reduction reaction on the cathode [11].

In an ongoing research on PEM fuel cell degradation at our own facilities, the applicability of the EIS technique for cell's health assessment was tested, with special attention being paid to the interpretation of inductive loops appearing at low frequencies. With that being said, a single PEM fuel cell has been exposed to an accelerated stress test (AST), and diagnostic tests (including the EIS) have been performed regularly throughout the experiment. Notably, experimental data from the EIS measurements were then used for a novel approach in the impedance model fitting. More specifically, a new, upgraded equivalent circuit with additional elements, of which each of them has a well-defined physical meaning, has been proposed and fitted against the experimental results. Furthermore, the values of each element obtained this way throughout the degradation experiment, were then extracted and analyzed to see whether their changes with time are in accordance with the expected behavior of the assigned physical meaning.

2. Model Description

A standard, simple representation of the fuel cell processes by equivalent circuits involves resistance/capacitance loops (representing activation losses on both anode and cathode) in series with a resistance (representing both ionic and electrical resistance in the membrane and cell hardware). Very often, this is simplified even further by neglecting anode's contribution,

and the resulting equivalent circuit (Randles circuit) is shown in Figure 1 a). In addition, a porous bounded Warburg element based on finite diffusion processes occurring through a fixed diffusion layer thickness, is so often added to represent mass transport losses at lower frequency region (capacitive loop at the right side of the Nyquist plots), Figure 1 b). However, such a model cannot explain the appearance of an inductive loop at low frequency.

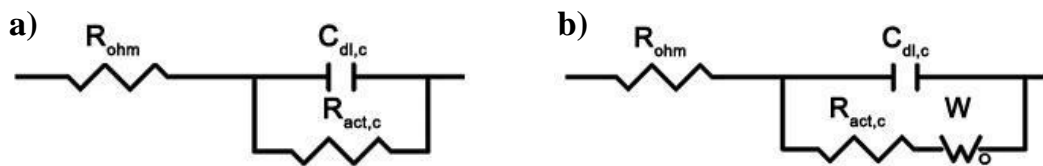


Figure 1. Randles equivalent circuit: a) simple, with only ohmic and activation elements, b) with Warburg element added.

In an attempt to explain the origin of the low frequency loops and correlate this with the processes within the fuel cell, a novel impedance model of a PEM fuel cell represented by a modified equivalent circuit has been proposed and validated. The proposed model takes into account both the anode and the cathode, and has an additional loop, comprising of a resistance, capacitance and inductance in parallel, added on either side forming the so called resonant loop. The proposed equivalent circuit is shown in Figure 2.

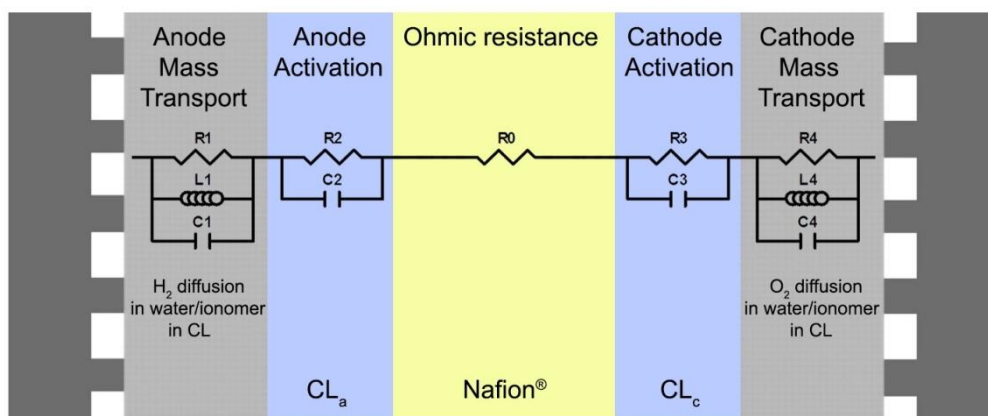


Figure 2. The proposed equivalent circuit with an approximate schematic representation of the relationship between the fuel cell geometry and the proposed equivalent circuit.

The added resonant loops represent the mass transport and resistive losses within the catalyst layer (CL) and gas diffusion layer (GDL). In this case, the physical processes preceding the

FB – Analysis of Degradation Mechanisms



catalytic reaction that take place in a complex structure of the fuel cell catalyst layer are represented by their electrical equivalents. Namely, inductance represents inertia of reactant gas (oxygen on the cathode and hydrogen on the anode), absorption and dissolution in water present in polymer; resistance represents not only protonic resistance through polymer within the catalyst layer, but also the resistance to transport (diffusion) of gas through water to the catalyst site; and capacitance represents stored (dissolved) quantity of gas within the water present in polymer.

3. Experimental

A single PEM fuel cell with a 50 cm² active area MEA, produced by BASF (12E-W MEA), has been subjected to an accelerated stress test designed to target electrocatalyst degradation. The cell was exposed to a 49 seconds long potential cycling profile, with rest voltages 0.6 V and 0.9 V, modeled on the recommendations from the Department Of Energy AST protocol for electrocatalyst degradation. The voltage was imposed on the cell via external instrument as the cell was in a non-operating mode, i.e. nitrogen was used in the cathode compartment (hydrogen was used on the anode side). A more detailed description of the AST protocol and the experiment is reported in [12]. Since the chosen operating conditions and the load profile were purposely very harsh, the whole experiment took only 5000 cycles (or ~68 hours) before it was halted, as the cell was deemed to degrade too much. The diagnostic tests were done at the beginning of life (BOL), after 1000, 3000 and 5000 cycles. Different diagnostic techniques were applied, however, only the EIS measurements are of the relevance for the analysis presented here.

The EIS tests were done at the cell temperature of 65 °C, with inlet relative humidities (RH) of 83.4% (dew point of 61 °C) for both hydrogen on the anode, and air on the cathode. Reactants flows were set at constant stoichiometry of 2 on the anode and 4 on the cathode, while the backpressures were the same for both compartments, 0.5 bar(g). All the recordings were conducted at the current density of 0.1 A/cm². The measurement itself was conducted in a galvanostatic mode (i.e. the current has been imposed on the cell and the voltage response was measured) in the frequency range from 3.981 kHz to 0.1 Hz. The frequencies were spaced in a logarithmic progression with ten points per frequency decade. Each scan took around 7 minutes and there was a 5 minute stabilization phase prior to each testing at the operating conditions, in order for the cell to reach the steady-state.

The AC signal amplitude was selected to be 10% of the DC current. In the EIS measurements, it is clear that the larger the AC perturbation amplitudes, the easier the separation of the measured response from noises, but also the signal amplitude has to be small enough to satisfy the linearity assumption. According to the study conducted by Dale et al. [13] on the impedance spectra, which also showed that the spectrum is very scattered for low load



currents (because it becomes difficult for a frequency response analyzer to distinguish between the response and noise), there is no considerable difference between the impedance plots in the amplitude range of 5%-10% of the DC performance current.

4. Application of model to fuel cell degradation study

Before the application of the proposed model to the fuel cell degradation test, for condition monitoring and health assessment, the model was first validated on another single cell which was the same as the one from the degradation test. The model was validated by fitting the measured impedance spectrum of the cell at 0.3 A/cm^2 , with all the other operating parameters the same as in the degradation test, except for the RHs which were 100% in this case. The lower frequency limit was set to 0.01 Hz in this case, so it took around 30 minutes to complete a scan. The other scan parameters were the same as in the degradation test.

The fit was obtained using Z Fit numeric tool from Bio-Logic EC-Lab[®] software. As shown in Figure 3, a very good agreement between simulation and measured data was achieved, including the low frequency inductive loop. The leftmost real-axis intercept (the high frequency intercept) point on the diagram represents the ohmic loss in the cell. This loss takes into account ionic losses in the membrane and the electrical (both electronic and contact) losses in cell hardware, but not the ionic losses within the catalyst layer. A tilted/distorted high frequency branch of the semicircle indicates ionic resistance in the CL. Decreasing the frequency (from left to right in the diagram), the low frequency inductive loop starts to appear around $\sim 5 \text{ Hz}$. The plot crosses the real-axis at $\sim 0.3 \text{ Hz}$ and then, with further decrease in frequency, circles back towards the real-axis. The final real-axis intercept (at $\sim 0.33 \text{ } \Omega \text{ cm}^2$), so called DC point, was calculated from the polarization curve slope at the measured current density (0.3 A/cm^2), and, as it can be seen in the diagram, its value extrapolates the plot perfectly.

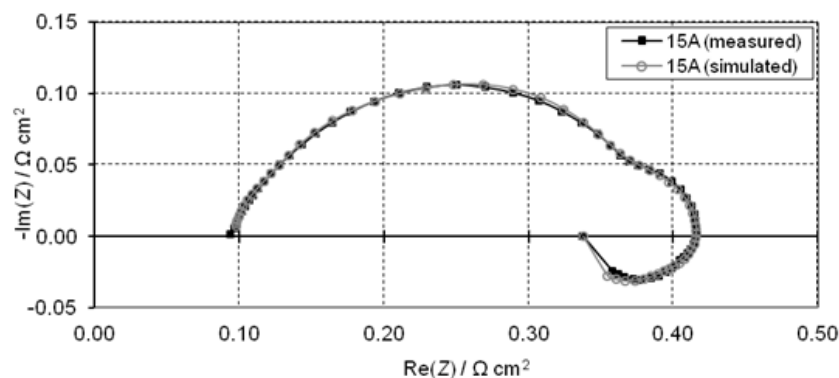


Figure 3. Comparison of Nyquist plots of measured and simulated impedance data at 0.3 A/cm^2 (15 A).



On Figure 4 the Nyquist plots of the cell subjected to the accelerated degradation test are shown. The diagram clearly shows performance deterioration with time (i.e. number of cycles): the semicircles' high frequency branches are getting more pronounced, indicating an increase in the CL ionic resistance, while the low frequency loops, representing mass transport losses, are getting bigger and in the end it is difficult to tell the two semicircles apart. As a result, the total resistance of the cell increased dramatically. From the plot it is obvious that the high frequency intercept, indicating ohmic losses, increased only in the first 1000 cycles (by ~30%), while remained more or less the same for the remainder of the degradation test. This concurs with the findings of other diagnostic tests (polarization curves and cyclic voltammetry) which also indicated a big loss of the cathode electrochemical active surface area (ECSA), almost 80% by the end of the test. The loss of the ECSA apparently resulted in big structural changes within the CL, as the increase in mass transport suggests.

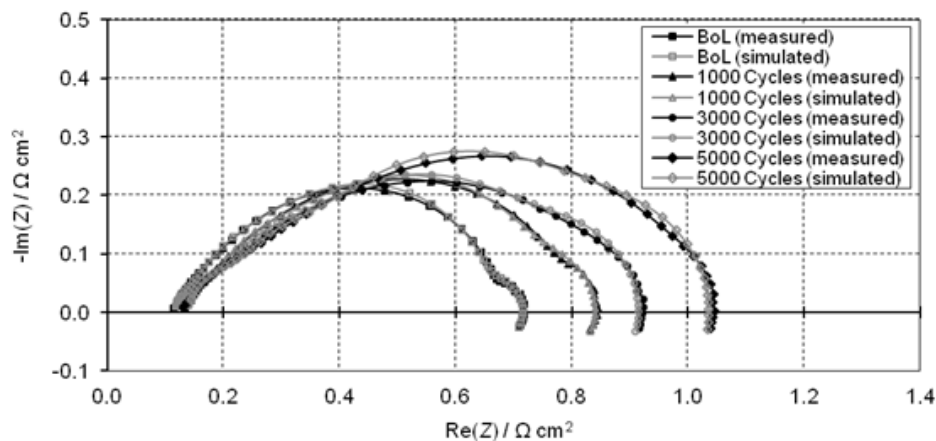


Figure 4. Comparison of Nyquist plots of measured and simulated impedance data at 0,1 A/cm² at different steps of the accelerated stress test.

The previously described model was fitted to the obtained EIS spectra in order to give more insight into cell's degradation. As shown in Figure 4, again a very good agreement to the experimental data was obtained. This enabled quantification of individual model components and the change of their values during the degradation experiment. Comparison of measured and simulated values of the ohmic resistance shows an excellent match throughout the degradation experiment, Figure 5.

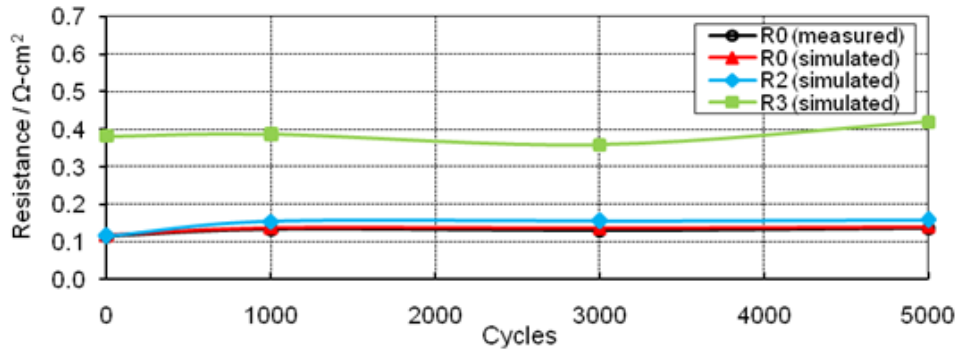


Figure 5. Comparison of measured and simulated values of the ohmic resistance (R0) and simulated activation resistances (R2 and R3) during the accelerated degradation test.

The model results also indicate that both the anode and cathode activation (charge transfer) resistances, R2 and R3 respectively, did not change significantly during the degradation test, and are more or less constant. These are actually realistic findings and they add to the validity of the model assumption that the R2 and R3 elements represent the assigned physical meaning. Even though this may seem illogical at first glance, the activation resistances should indeed remain more or less constant despite the significant degradation of the CL. With the CL degradation and consequent loss of ECSA, activation losses increase, but the activation resistance, i.e. $(\partial U / \partial i)_{act}$, at the same current density (and temperature, obviously) should theoretically remain the same, as the reaction kinetics should not change with degradation. Additionally, the model results indicate that the cathode activation resistance is about 2–2.5 times higher than the one on the anode, which is also in accordance with theory. Thus, one can conclude that the model managed to isolate contributions of both, cathode and anode activation resistance in overall cell resistance pretty accurately.

Figure 6 shows the comparison between the simulated values for the anode and cathode mass transport resistance.

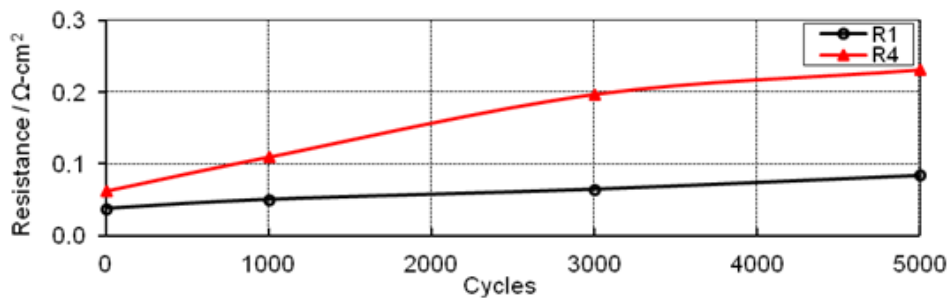


Figure 6. Comparison of simulated values of the mass transport resistances (R1 and R4) during the accelerated degradation test.



It is evident that initially both values are rather small, but still the cathode value is somewhat higher, which is expected as oxygen diffusion through catalyst layer is slower than hydrogen diffusion. Also, the cathode's mass transport resistance increases much faster with the degradation, as expected since the degradation test was designed to aim the cathode catalyst layer. Not only did the oxygen diffusion increase due to structural changes within the CL, but also the ionic resistance through the ionomer in the CL increased due to the degradation.

Similarly, the cathode catalyst layer inductance, L4, is initially higher and increased more dramatically during the degradation than the anode one, L1, as shown in Figure 7. As explained earlier, newly introduced inductance element, represents inertia of the reactant gases to dissolve in water/ionomer present in the CL. One would expect that the cathode inductance is initially higher than the anode one, since the oxygen molecule is much bigger and dissolves slower in water/ionomer than the hydrogen molecule. The faster increase in the cathode inductance with the degradation was also expected as the degradation test targeted cathode CL, which impedes oxygen dissolution.

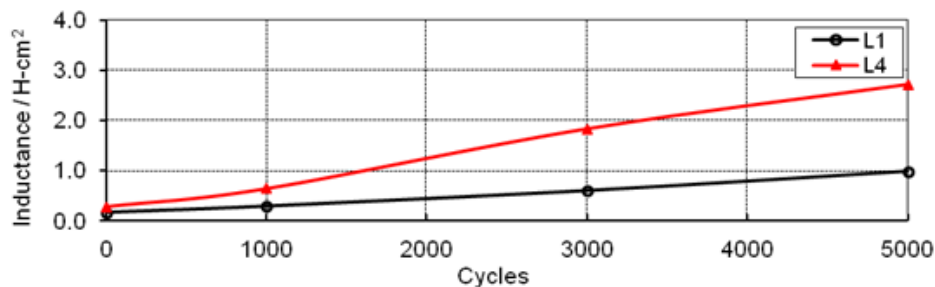


Figure 7. Comparison of simulated values of the mass transport inductances (L1 and L4) during the accelerated degradation test.

The catalyst layer capacitances (double layer capacitances), C2 (representing the anode) and C3 (representing the cathode), did not change significantly during the degradation test, as shown in Figure 8. Since the cathode activation polarization is significantly higher than the anode, C3 values are also higher than C2 values.

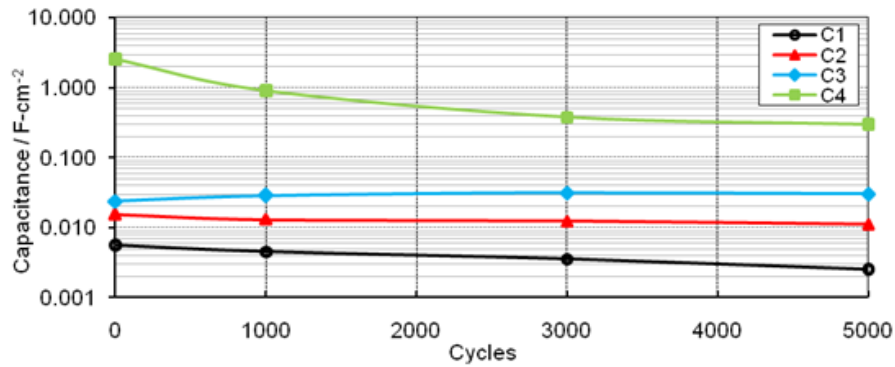


Figure 8. Comparison of the simulated values for the model capacitances during the accelerated degradation test.

However, the cathode catalyst layer capacitance, C4, representing capacitance of oxygen in water/ionomer in the cathode catalyst layer, decreased by an order of magnitude over the duration of the degradation test. This behavior was expected in correlation with the cathode inductance increase due to the cathode CL degradation. On the other hand, the anode catalyst layer capacitance, C1, which is initially about two orders of magnitude lower than the cathode one, decreased only slightly with the degradation.

In Figure 9 a comparison of measured and simulated total resistances is shown. The total resistance represents the sum of all resistances in the proposed model ($Total R = R_0 + R_1 + R_2 + R_3 + R_4$) and can be used for model validation. Measured values of the total resistance are obtained from the low frequency intercepts of impedance response and the real-axis. As it can be seen, there is an excellent agreement between simulated and experimentally obtained values.

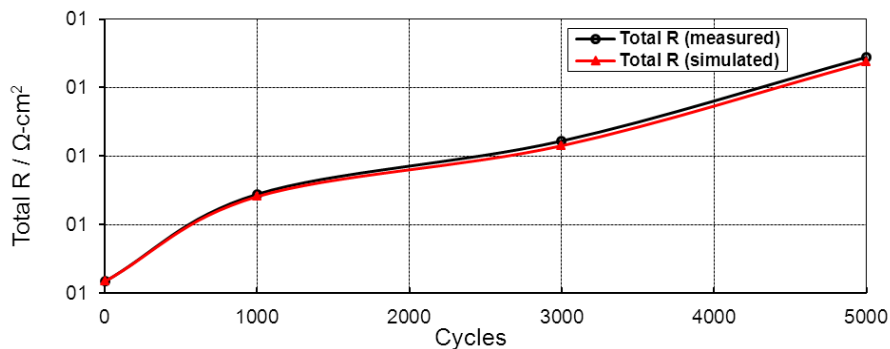


Figure 9. Comparison of measured and simulated values of the total resistance during the accelerated stress test.



5. Conclusions

A new equivalent circuit model, that involves two resonant loops, and which can fit the low frequency inductance loops observed in PEM fuel cells electrochemical impedance spectroscopy experiments, was introduced and tested as a tool for condition monitoring and health assessment of PEM fuel cells. Since each of the elements of the proposed equivalent circuit has a clearly defined physical meaning (i.e. it is clearly related to different properties and phenomena in the cell), it is possible to quantify each of them and monitor their changes over time. Validations of the model showed excellent agreement with experimental results, and therefore it can be concluded that the model actually gives pretty accurate picture of the processes that take place in a complex catalyst layer structure.

This approach was used to monitor the state of health of a PEM fuel cell exposed to an accelerated degradation test consisting of frequent voltage cycling. The cell degraded very fast and the model managed to extract contributions of different phenomena responsible for the cell degradation, which were in accordance with the expected behavior, regarding their physical interpretations. Namely, activation resistances remained the same throughout the experiment on both sides (anode and cathode) and their relative sizes were in accordance with the literature. As for the newly presented resonant loop, all the elements of the cathode loop (except the capacitance) were initially slightly higher and increased much faster with the degradation than the elements of the anode loop. The cathode capacitance, representing the quantity of dissolved oxygen in water/ionomer in the CL, was initially two orders of magnitude higher than the anode counterpart, and decreased tremendously with the degradation.



References:

- [1] R. O'Hayre, S. Cha, W. Colella, F. B. Prinz: "Fuel Cell Fundamentals", John Wiley & Sons, Inc., Hoboken, New Jersey, 2009.
- [2] E. Barsoukov, J. R. Macdonald: "Impedance Spectroscopy: Theory, Experiment, and Applications", John Wiley & Sons, Inc., Hoboken, New Jersey, 2005.
- [3] M. E. Orazem, B. Tribollet: "Electrochemical Impedance Spectroscopy", John Wiley & Sons, Inc., New Jersey, 2008.
- [4] X.-Z. Yuan, C. Song, H. Wang, J. Zhang: "Electrochemical Impedance Spectroscopy in PEM Fuel Cells: Fundamentals and Applications", Springer, 2010.
- [5] A. S. Arico, V. Alderucci, V. Antonucci, S. Ferrara, V. Recupero, N. Giordano, K. Kinoshita, *Electrochim. Acta* 37 (1992) 523.
- [6] O. Antoine, Y. Bultel, R. Durand, *J. Electroanal. Chem.* 499 (2001) 85.
- [7] S. K. Roy, M. E. Orazem, B. Tribollet, *J. Electrochem. Soc.* 154 (2007) B1378.
- [8] P. Piela, R. Fields, P. Zelenay, *J. Electrochem. Soc.* ,153 (2006) A1902.
- [9] S.-I. Pyun, Y.-G. Ryu, *J. Power Sources*, 62 (1996) 1.
- [10] I.A. Schneider, M.H. Bayer, A. Wokaun, G.G. Scherer, *J. Electrochem. Soc.* 155 (2008) B783.
- [11] N. Holmström, K. Wiezell, G. Lindbergh, *J. Electrochem. Soc.* 159 (2012) F369.
- [12] D. Bezmalinović, F. Barbir, "Analysis of Degradation Mechanisms", SAPPHIRE project (FP/2007-2013, n° 325275) deliverable 5.1,
<https://sapphire-project.eifer.kit.edu/images/pub/D5.1.pdf>
- [13] N. V. Dale, M. D. Mann, H. Salehfar, A. M. Dhride, T. Han, *J. Fuel Cell Sci. Technol.* 7 (2010) 031010.